LES AND URANS COMPUTATIONS OF 3D NATURAL CIRCULATION LOOPS

D. R. Wilson[1*], H. Iacovides[1], T. J. Craft[1]

[1]Department of Mechanical, Aerospace and Civil Engineering, University of Manchester, Manchester M13 9PL, United Kingdom

ABSTRACT

Natural Circulation Loops (NCL) offer potential for use in passive cooling systems within nuclear power plants. The combination of uniform heat flux at the hot end and uniform temperature at the cold side promotes thermal imbalances which can cause flow instabilities that severely challenge numerical methods. This study employs both unsteady RANS and Large Eddy Simulation (LES) for the conjugate heat transfer analysis of an experimental NCL across a range of different heating powers, with a focus on comparing several widely used URANS models (Launder-Sharma $k-\varepsilon$, $k-\omega$ SST, and Elliptic-Blending RSM) against the higher-fidelity LES. The results indicate that the EB-RSM marginally outperformed the LS $k-\varepsilon$, with the latter demonstrating good agreement with experimental data across a wide range of powers. The $k-\omega$ SST model performed less well, tending to overpredict turbulence levels within the loop, leading to higher heat transfer coefficients and significantly cooler temperatures. Overall, the results demonstrate the suitability of the CFD approach in modelling NCLs.

1 INTRODUCTION

A Natural Circulation Loop (NCL) is a closed circuit in which fluid is driven solely by thermal imbalance. Such passive systems are expected to feature extensively in the development of new Generation IV nuclear reactor concepts, owing to their potential to contribute towards the safety and simplification of plant and reactor design. Despite being geometrically simple, the combination of uniform heat flux at the hot end and uniform temperature at the cold end promotes thermal imbalances which can cause large-scale flow oscillations, including flow reversal. The flow analysis is further complicated by both the influence of heat conduction through the pipe walls and, as is common in flows dominated by natural convection, the possible coexistence of laminar, turbulent and transitional regions at different locations around the loop. This wide and complex range of flow behaviours presents severe challenges to the reliable numerical simulation of such loops.

Whilst very little 'CFD grade' experimental data is available in the open literature, an example of typical NCL behaviour is provided by a loop located at the Bhabha Atomic Research Centre (BARC), India [1]. This is a uniform diameter rectangular water-based loop with two heaters and two coolers, providing four different heating configurations across a range of heating powers ($0 < Q_h$ [kW] < 1). Experiments covered both steady-state behaviour and start-up transients. For the most stable configuration, with a vertically oriented heater and cooler (VHVC), stable flow was observed across the entire power range considered, providing an ideal case to assess the capabilities of current CFD modelling methodologies. Our previous work [2] solved a simplified 2D NCL and demonstrated that an Unsteady Reynolds-averaged Navier-Stokes (URANS) approach was able to predict both unstable behaviour, qualitatively similar to that reported experimentally, and steady-state behaviour in agreement with existing correlations [3].

To further assess the capabilities of CFD codes in reproducing complex natural convection thermal-hydraulic phenomena, and extend our previous work to three-dimensions, this study employs both URANS and LES for the conjugate heat transfer analysis of the BARC NCL in the most stable configuration (VHVC). First, to help address the lack of highly detailed flow data, and provide a high fidelity reference to compare the RANS against, we conduct a LES of the highest power case ($Q_h = 1$ kW). Second, we then perform simulations using a range of RANS turbulence models and turbulent heat flux models, with an aim to assess the performance and suitability of these more readily accessible

*Corresponding Author: dean.wilson@manchester.ac.uk

methodologies in reproducing both overall system behaviour and local flow phenomena. Finally, we apply one of the RANS models across a representative subset of the heater powers considered in the experiment.

2 NUMERICAL METHODOLOGY

2.1 Analysis of NCLs

By considering a one-dimensional form of the governing equations (continuity, momentum and energy) around the loop, and assuming a steady state exists, Vijayan [3] provides a solution of this coupled system of equations in non-dimensional form. The result is a relation between the modified Grashof number Gr_m (as the primary input) and the steady state Reynolds number Re_{SS} of the flow around the loop that results (i.e. the output):

$$Re_{SS} = C\left(\frac{Gr_m}{N_g}\right)^r \tag{1}$$

where C and r are constants which depend upon the flow condition, as per Table 1 . The steady state Reynolds number, Re_{SS}, the modified Grashof number, Gr_m, and the geometric parameter N_g are defined as:

$$Re_{SS} = \frac{D\dot{m}_{SS}}{A_c\mu}, \quad N_g = \frac{L_t}{D} \tag{2}$$

$$Gr_m = \frac{D^3\rho^2\beta g\Delta T_r}{\mu^2}, \quad \Delta T_r = \frac{Q_h\Delta Z}{A_c\mu c_p} \tag{3}$$

where D is the pipe diameter [m], ρ is the fluid density [kg m^{-3}], β is the volume expansion coefficient [K^{-1}], g is acceleration due to gravity [m s^{-2}], μ is the fluid viscosity [Pa s], ΔZ is the vertical elevation difference between the centre of the heater and cooler [m], Q_h is the power provided by the heater [W], c_p is the specific heat capacity [J kg^{-1}K^{-1}], L_t is the centreline length of the loop [m] and A_c is the cross-sectional area of the pipe [m^2]. Equation 1 has demonstrated excellent agreement across a wide range of experimental loops [3].

Table 1: Constants for Equation 1, applicable for different flow conditions [3].

Flow condition	C	r
Laminar	0.1768	0.5
Turbulent	0.196	1/2.75
Transitional	0.3548	0.43

2.2 Case description and meshing

We consider here only the vertical heater vertical cooler (VHVC) configuration of the BARC loop since, being the most stable, it is an ideal case for an LES computation owing to a well-defined steady state. A schematic of the loop considered is presented in **Error! Reference source not found.**. The heater can provide a uniform heat flux (such that $0.1 < Q_h$ [kW] < 1) whilst the cooler comprises a coaxial heat exchanger with the secondary coolant (water) flowing through an annulus, modelled as providing a uniform wall temperature ($T_c = 34$ ℃). Due to the expected influence of the pipe walls, a full conjugate heat transfer approach is applied taking into account the properties of the borosilicate glass walls present in the experiment. In the experiment, the mass flow rate ($\dot{m}_{SS}$) was estimated by applying an energy balance across the heater, using thermocouple measurements upstream and downstream to obtain a representative temperature difference. For consistency, the same approach is applied when processing the CFD results. The initial temperature is the same as the cooler temperature.

Block structured meshes comprising hexahedral elements are utilized, with a low-Re wall modelling approach applied for all models tested. Following mesh sensitivity tests, two meshes were produced

using the ANSYS ICEM-CFD (v19.2) package with cell counts ranging from 27 million for the LES, to 2.6 million and lower for the RANS. A representative image of both meshes is presented in **Figure 1**. Quality tests on the LES mesh (not shown here) show that, on average, 99.8% of cells have a sub-grid-scale to total turbulent kinetic energy ratio of $k_{sgs}/k_t \leq 0.2$.

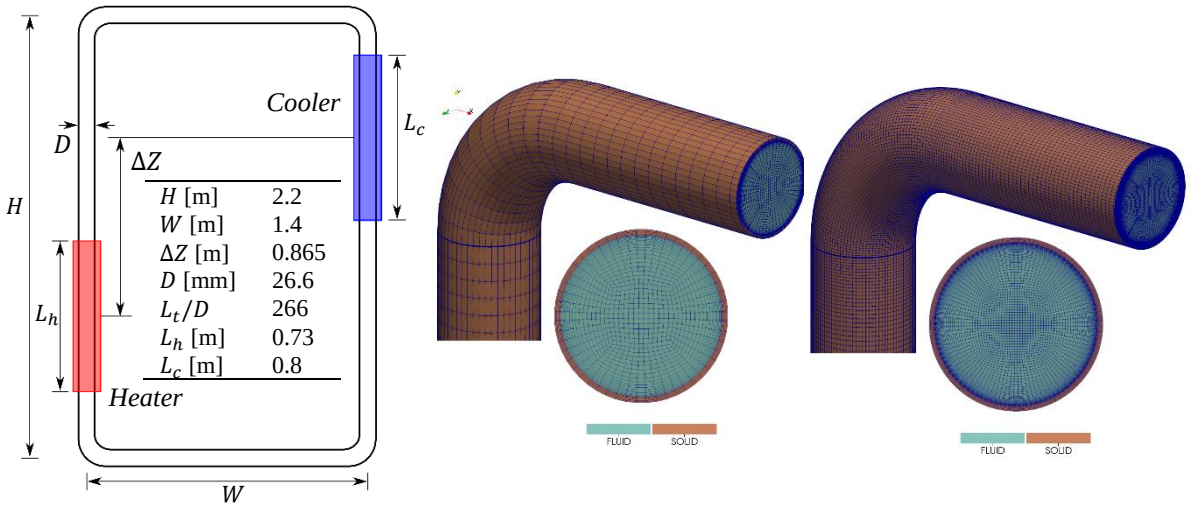

Figure 1: Schematic of the loop with geometric dimensions (left) and representative images of the mesh employed for the URANS (middle) and LES (right).

2.3 Turbulence modelling

For the LES, which solves filtered forms of the continuity, momentum and temperature transport equations, the effects of the small-scale fluctuations, removed by the filtering operation, are provided by the Wall Adapting Local Eddy viscosity (WALE) sub-grid-scale model. This extends the popular Smagorinsky model by relating the eddy-viscosity to the local rotation rate in addition to the local strain rate. It is also designed to return the correct near-wall behaviour without the use of any damping functions. For the URANS, we apply the Launder-Sharma (LS) variant of the $k-\varepsilon$ model, the $k-\omega$ SST, and the Elliptic-Blending Reynolds Stress Model (EB-RSM), all extended with the appropriate buoyant generation terms. The Simple Gradient Diffusion Hypothesis is used with the eddy-viscosity models whilst the General Gradient Diffusion Hypothesis is used with the RSM. Transient computations are performed using the open-source *Code_Saturne* v6, with temperature dependent properties and a time-step chosen such that the CFL number remains at or below 1. Results are time-averaged once a statistically steady-state has been achieved.

3 RESULTS

3.1 Long-term averaged velocity and temperature profiles

First, we present comparisons of the four different modelling approaches employed at the highest power considered ($Q_h = 1$ kW). All models produced stable steady-state flow as expected, since in the VHVC configuration a strong preferential direction is imposed by both heat exchangers. **Figure 2** presents long-term time-averaged velocity and temperature profiles at the exit of the heater and cooler. The EB-RSM demonstrates excellent agreement with the LES, correctly picking up the buoyancy-driven near-wall velocity peaks at the exit of both the heater and the cooler. This is likely due to its ability to better capture anisotropy in the turbulence, something that buoyancy is known to induce. The shifts in the temperature profiles occur due to the models' differing predictions of mean loop temperatures, which are a result of differences in the resultant heat transfer coefficients within the heat exchangers (see Table 2).

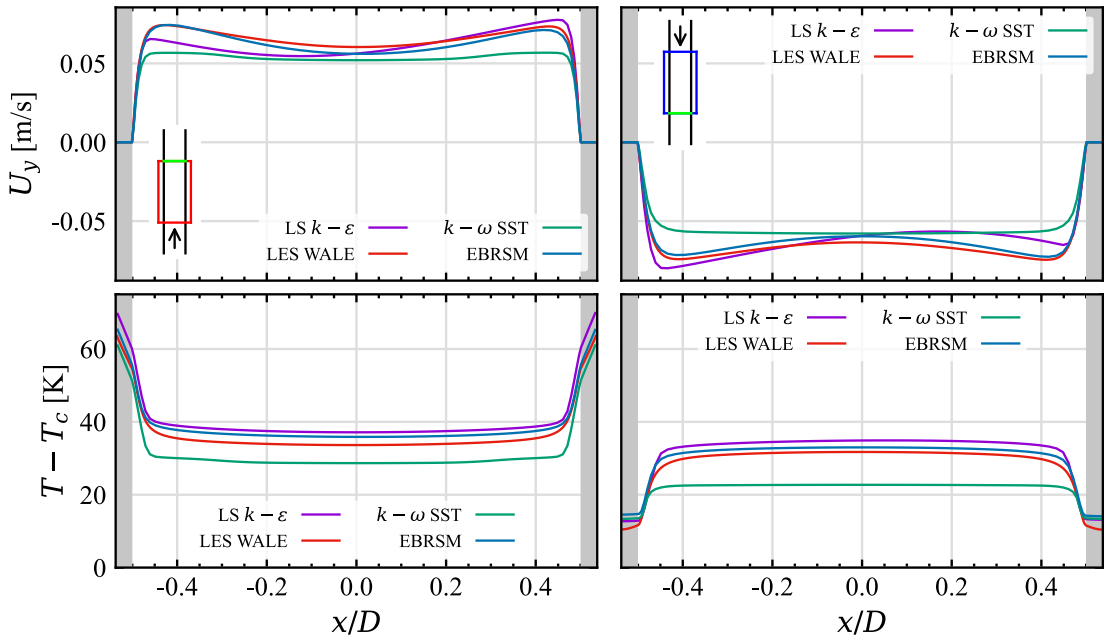

Figure 2: Long-term time-averaged vertical velocity (top) and temperature (bottom) profiles at the exit of the heater (left) and cooler (right) for all modelling approaches tested. The grey regions either side represent the pipe walls.

Table 2: Comparison of selected time-averaged flow statistics between the experiment [1] and present CFD simulations at $Q_h = 1$ kW. T_m is the volume averaged temperature within the loop, $\Delta T_h$is the temperature drop across the heater and the mass flow rate, $\dot{m}_{SS}$ is computed using an energy balance as discussed in Section 2.2.

Model	T_m [K]	ΔT_h [K]	$\dot{m}_{SS}$ [kg s^{-1}]	h_c [Wm^{-2}K]	Gr_m	Re_{SS}
EXP	345.53	6.47	3.745E-2	N/A	7.110E11	4.574E3
LS $k-\varepsilon$	343.12	5.73	4.229E-2	586.04	6.231E11	4.958E3
$k-\omega$ SST	333.31	6.85	3.541E-2	932.85	3.707E11	3.605E3
EB-RSM	341.56	6.08	3.987E-2	620.35	5.761E11	4.574E3
LES WALE	339.91	5.31	4.567E-2	670.37	5.268E11	5.114E3

With the LS $k-\varepsilon$ model, the velocity profiles (Figure 2) show a slight increase in asymmetry within both heat exchangers but are in better agreement with the LES than the $k-\omega$ SST, which predicts much flatter velocity profiles and notably cooler temperature profiles. Both of these discrepancies can be traced to the prediction of much higher turbulence levels by the $k-\omega$ SST within the interconnecting pipe sections of the loop, which leads to increased heat transfer coefficients within the cooler and therefore much cooler overall temperatures (as shown in Table 2). This is demonstrated in Figure 3, which plots the long-term time-averaged turbulent kinetic energy and temperature along the loop centreline for all models tested. Despite the absence of any significant turbulence production within the heat exchangers, the failure of the $k-\omega$ SST to correctly capture the reduction in turbulence outside those regions (compared to the LES) means that the flow becomes strongly turbulent in the interconnecting pipes. This results in much higher turbulence levels at the inlets of both heat exchangers, leading to increased mixing of the thermal fields and a more immediate (and linear) change in centreline temperature throughout the heat exchangers compared to the other approaches. This increased mixing quickly flattens the near-wall velocity peaks which would have been generated by the buoyancy force (see Figure 2) as the flow enters either heat exchanger.

The reason for the above difference in turbulence levels is most likely due to the absence of specific low-Re damping terms, present in both the EB-RSM and LS $k-\varepsilon$, which are designed to reduce turbulence in regions where viscous forces become influential. Whilst there are forms of the $k-\omega$ part of the $k-\omega$ SST which include some damping functions [4], they are not included within *Code_saturne* as they were found to cause significant stability issues in other flows. With the other two RANS models,

the LS $k-\varepsilon$ and the EB-RSM, the k profiles do also highlight some quantitative differences when compared with the LES, with both tending to underpredict the influence of the bends whilst overpredicting the influence of the heater. The EB-RSM in particular underpredicts the increase in k generated by the elbows.

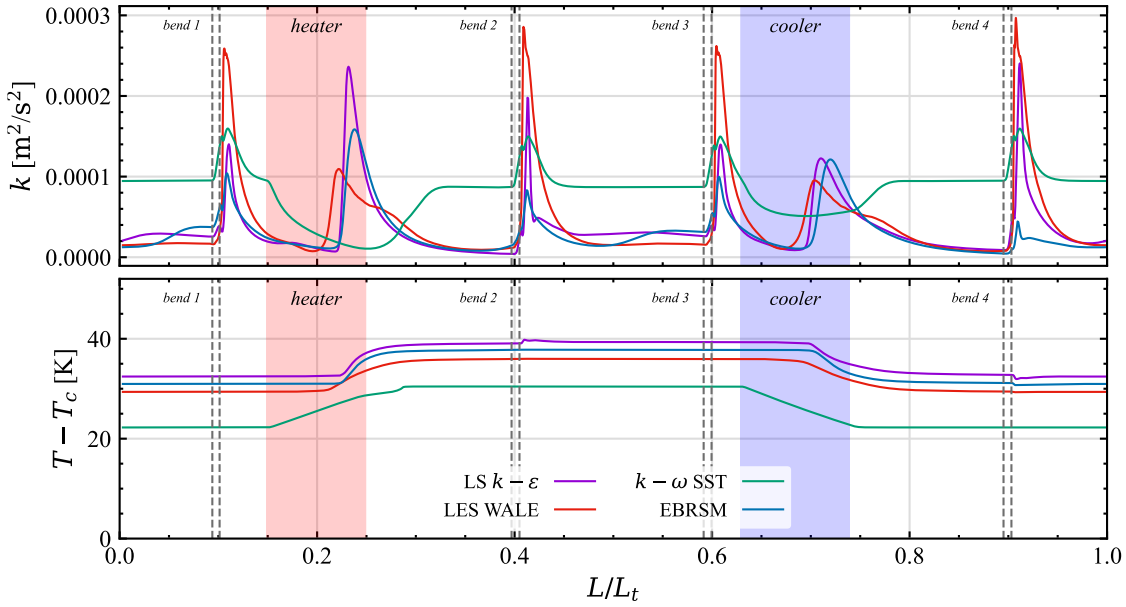

Figure 3: Long-term time-averaged total turbulent kinetic energy (top) and temperature (bottom) profiles along the pipe centreline for all modelling approaches tested.

3.2 Integral quantities and LS $k-\varepsilon$ performance across full power range

Figure 4 plots the Reynolds number (Re_{SS}) of the resulting statistically steady flow around the loop against Gr_m/N_g for all cases modelled. Comparisons are drawn against both the experimental results and the simplified analysis presented by Vijayan [1] (see Section 2.1). The application of the LS $k-\varepsilon$ model to a wide range of powers ($0.1 < Q_h$ [kW] < 1) demonstrates excellent agreement with the trends suggested by both the experimental and the correlation. Despite their good agreement with the turbulent correlation, results at powers $Q_h < 650$ W returned laminar flow.

At the highest power considered ($Q_h = 1$ kW), highlighted inset on Figure 4, the $k-\omega$ SST predicted a noticeably lower Re_{SS} and Gr_m that other approaches, due principally to the previously discussed overprediction of turbulent levels around the loop. This leads to much cooler overall temperatures, which reduces Gr_m through the dependence of properties on temperature, and an increased temperature drop across the cooler, which means that a smaller mass flow rate (and thus Re_{SS}) is required for thermal equilibrium between the heater and cooler. Despite these differences, and despite a number of differences in the prediction of the flow fields, all four modelling approaches produce Re_{SS} and Gr_m values in relatively good agreement with the correlations. This is not particularly unexpected, because all approaches can satisfy the principles of mass, momentum, and energy conservation that Equation 1 is derived from. Consequently, whilst agreement with the correlation is a necessary condition for a simulation to be valid, it is not a sufficient one, and it cannot be used to directly infer the accuracy of the flow fields themselves.

4 CONCLUSION

The statistically steady flow within an experimental Natural Circulation Loop has been reproduced with three different URANS approaches and complementary LES. Comparisons between the approaches revealed that the Launder-Sharma $k-\varepsilon$ model provides reasonable agreement when compared with the more advanced EB-RSM. The $k-\omega$ SST model tended to overpredict turbulence levels within the loop, leading to significantly cooler temperatures, higher heat transfer coefficients and flatter velocity profiles;

something attributed to the lack of low-*Re* damping terms in the version implemented in *Code_saturne*. Although all approaches demonstrated agreement with the correlations, we caution against using such agreement to infer accuracy of the flow fields themselves. Application of the LS $k-\varepsilon$ to a wide range of heater powers demonstrated good agreement with the trends presented by both the experimental data and existing correlations. Further interrogation of the LES dataset is planned, to provide additional in-depth assessment of the URANS approaches employed here.

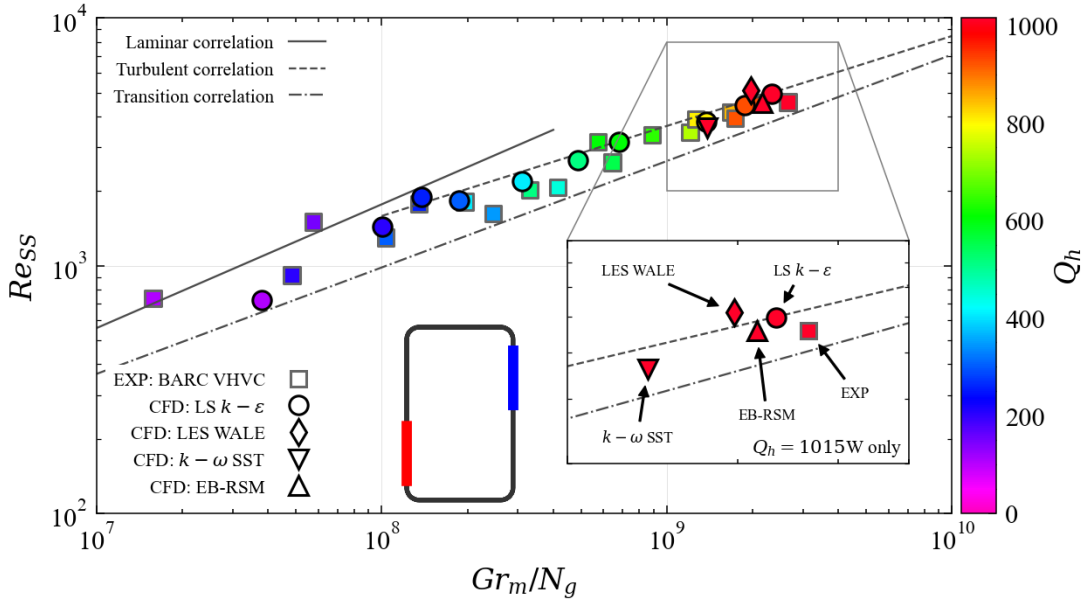

Figure 4: Steady-state Reynolds number Re_{SS} against the modified Grashof number Gr_m scaled with N_g for the BARC NCL [1]. The correlations plotted are from Equation 1 with constants as per Table 1. The symbol colour indicates the heater power, Q_h, as per the colour bar on the right. Inset provides a comparison at a single power, $Q_h = 1$ kW, for all models tested together with the equivalent experimental datum.

ACKNOWLEDGEMENTS

This research has been conducted as part of the UK Nuclear Innovation programme, funded by the UK Department of Business, Energy and Industrial Strategy. We greatly acknowledge the support and use of Scafell Pike at the Science and Technology Facilities Council and the CSF at the University of Manchester.

REFERENCES

[1] Vijayan, P.K., Bhojwani, V.K., Bade, M.H., Sharma, M., et al., Investigations on the effect of heater and cooler orientation on the steady state, transient and stability behaviour of single-phase natural circulation in a rectangular loop, Bhabha Atomic Research Centre, 2001.

[2] Wilson, D., Iacovides, H., Craft, T.J., Numerical insights into the transient behaviour of single phase natural convection loops for nuclear passive cooling applications, in: *Proceedings of 11th International Symposium on Turbulence and Shear Flow Phenomena*, Southampton, UK 2019.

[3] Vijayan, P.K., Experimental observations on the general trends of the steady state and stability behaviour of single-phase natural circulation loops. *Nucl. Eng. Des.* 2002, *215*, 139–152.

[4] Wilcox, D., A half century historical review of the k-omega model, in: *29th Aerospace Sciences Meeting*, American Institute of Aeronautics and Astronautics, 1991.